

23rd World Gas Conference, Amsterdam 2006

**MEASUREMENT OF GAS CALORIFIC VALUE:
A NEW FRONTIER TO BE REACHED WITH AN OPTIMISED
REFERENCE GAS CALORIMETER**

C. Villermaux¹, M. Zarea¹, F. Haloua², B. Hay², J.-R. Filtz²

¹ Gaz de France, (GdF), R & D Division, BP33, St Denis La Plaine Cedex, France, 93211

² Laboratoire national de métrologie et d'essais (LNE), 1 rue Gaston Boissier, Paris Cedex 15, France, 75724

ABSTRACT

Following European directives opening the gas market to competition, the precise measurement of the energy content of natural gas is now a strong need in order to better control costs across an increased number of interfaces, and to guarantee confidence in a context of increasing number of market players. Only a reference gas calorimeter can pretend to reach the lowest uncertainty on the gross calorific value (GCV) measurement.

We also present and discuss the past and current practices at Gaz de France for determining the gas GCV, and how these practices have evolved under the joint influence of new technologies (compact chromatographs, refined gas network simulation, etc.) and new standards and regulations.

Therefore, measurement of GCV on a large industrial scale is a significant issue, as it underlies billing. Opportunities for using more accurate reference calorimeters are also discussed, as one of the means to continue improving the standards of operation and customers' satisfaction. One way is to compare direct and indirect measurement methods, and the other one is to generate more recent data for the energy content of each gas component present in natural gases from different origins.

The European gas community, in association with LNE – French national metrology and testing institute, started a few years ago the development of a reference gas calorimeter. From a metrological point of view, but also in terms of social acceptability, it was recommended to build also additional reference gas calorimeters, in order to strengthen the first one. Consequently, another one is currently under development at LNE, in France. This paper describes an original approach of combining numerical simulation and experimental testing for optimising the calorimeter design, in order to improve its accuracy.

In order to optimise thermal homogeneity and maximize heat transfer to the water bath, which play the most important roles in terms of achieving an ambitious goal of 0.05% accuracy, Gaz de France performed detailed transient 3D numerical simulations of the flow and heat transfer in the calorimeter bath, particularly checking the influence of the radiative heat transfer when compared to the imposed surface flux case, representative of the electrical heating during calibration. These simulations follow realistically all the three phases of each experiment, providing an insight that was not reported before in the operation of such a calorimeter over the whole measurement cycle.

We present here a comparison of experimental water bath temperatures as a function of time during calibration via electrical heating and actual measurement via combustion tests with results from the simulations with the CFD thermal model. The numerical model adequately reproduces the experimentally observed thermal behavior of the calorimeter. It helps point out differences in thermal non-homogeneity between the calibration and measurement modes, and provided, together with experimental results, evidence for locating the thermistance probe that is supposed to measure the average water bath temperature.

This first achievements of the combined experimental and numerical simulation approach will be developed in the future for other design aspects of the reference calorimeter, via even more realistic CFD models.

TABLE OF CONTENTS

1. Abstract
2. Introduction and background
3. Evolving practices for gas calorific value measurement in France
4. Applications of a reference gas calorimeter
5. Objectives of the study
6. Experimental and computational set-up
 - 6.1 Experimental set-up
 - 6.2 CFD Thermal model
7. Experimental and numerical results
 - 7.1 First experimental results
 - 7.2 Average temperature evolution
 - 7.3 Single thermistor position for measuring average bath temperature
8. Conclusion
9. References
10. List Tables
11. List of Figures

1. INTRODUCTION AND BACKGROUND

Following European directives opening the gas market to competition, the precise measurement of the energy content of natural gas is now a strong need in order to better control costs across an increased number of interfaces, and to guarantee confidence in a context of increasing number of market players. These new players include pipeline operators, now sometimes separated from storage and LNG receiving terminal operators, gas distributors, shippers, etc., that unlike before, need separate accounting and measurement systems. This new situation increases the number of points requiring the knowledge of physical parameters (delivered energy, etc), guaranteeing reliable performance at the lowest cost.

For this reason, the International Organisation of Legal Metrology (IOLM) is preparing a future recommendation concerning "Measuring systems for gaseous fuels", which covers volume, mass, and energy measurements for gaseous fuels. This draft recommendation defines three classes in terms of accuracy, based for instance on flow rate levels, with the corresponding levels of MPE – Maximum Permissible Errors. The MPE levels for gas calorific value (GCV) measurements are: ± 0.5 % in class A (largest flow rates), and ± 1 % in classes B and C (smaller flow rates).

As billing is based on delivered energy, the issue of measuring energy with the accuracy required by the IOLM recommendations, as well as the issue of a primary metrological reference for gas calorific value become high ranking priorities.

The first issue is covered in the present paper by a brief presentation of current and evolving operating practices of GRTgaz, the main French gas transmission operator, in order to adapt to the new requirements, while the second issue is illustrated by the high technology developments performed for the achievement of ambitious metrological goals for a gas reference calorimeter, developed by LNE, the French legal metrology institute, together with Gaz de France, and an European team, within a GERG (Groupe Européen de Recherche Gazière) collaborative project.

2. EVOLVING PRACTICES FOR GAS CALORIFIC VALUE MEASUREMENT IN FRANCE

In the past, Gaz de France used to manage GCV measurements at the supply points – borders and underground storages – using first calorimeters and chromatographs, and lately only gas chromatographs. Given the relatively "round" territory and gas supplies around the circumference, the French network is very meshed, inducing a quite significant number of GCV measurement points.

As the number of exchange points is going to increase, there is an opportunity for new technologies to evolve, like compact chromatographs, GCV measurement devices based on correlations, refined gas network simulation, etc. Gaz de France's R&D Division plays a key role in keeping pace with evolving technologies: the Gas Quality Laboratory evaluates the metrological performance of the most promising new products, both in the lab and in field tests.

Devices and methods used at transaction points need to be approved by the national legal metrology body, according to the IOLM recommendations.

Compact or micro chromatographs are now available, which are cheaper, have more limited analysis capacities, but are therefore quicker. They allow the reconstruction of the GCV from the measurement of gas composition, and the use of the GCV values given in the ISO 6976 standard. Class A accuracy on GCV can be achieved in most cases with these apparatus.

Competing devices are also proposed, based on the measurement of some physical parameters of gas, which are correlated to gas composition, hence to GCV. If these devices are more economical, their drawback is that their performance can degrade when the gas composition changes from the current range. Their performance spans classes A and B, according to conditions.

GCV can be also reconstructed via a technique based on using the commercial gas transmission network transient simulation software SIMONE, which was satisfactorily tested by

GRTgaz and GDF R&D Division under certain circumstances of network structure and instrumentation to be able to indicate / track the GCV value in a given area with class B accuracy. It represents an interesting and effective alternative to other class B approaches. This method needs the formal approval of the French legal metrology before it can be used for transactional purposes.

3. APPLICATIONS OF A REFERENCE GAS CALORIMETER

All the above-mentioned indirect measurement methods need data on the GCV of the individual components of natural gas. The currently used reference calorific values of natural gas components in the standard ISO 6976 [1] are matched with an uncertainty of at best $\pm 0.12\%$ (methane) and rely on measurements carried out between 1930 and 1970. The experimental procedure used at that time is not well known, what makes the uncertainty budget incomplete. Consequently, only a reference gas calorimeter can perform calorific value measurements with the lowest possible uncertainty. Calorific value measurements with an uncertainty lower than $\pm 0.1\%$ can be achieved with an isoperibolic calorimeter, where the water jacket is maintained at constant temperature.

Therefore, GERG (Groupe Européen de Recherche Gazière) initiated the development of a new up-to-date reference calorimeter, with a target measurement uncertainty of $\pm 0.05\%$, to be used among others, for generating new reference data, in order to update the ISO 6976 standard. Some features of this reference calorimeter of the Rossini, or isoperibolic type, were described in [2] and [3]. It is planned to have such calorimeters set up in Germany and France. The latter is being developed in parallel by Laboratoire National de Métrologie et d'Essais – LNE, with a specific contribution of Gaz de France's R&D Division to the optimisation of its design, which will be developed in the remainder of the paper. Both LNE and Gaz de France are partners in the GERG project.

More generally, such a reference calorimeter can be also used for checking reference gases used for calibrating chromatographs, as well as for evaluating the performance of any new indirect GCV measurement device or process in terms of national metrology. It contributes therefore significantly to accompany the current evolutions in the structures of natural gas markets. It is also important from the metrological point of view to have available several reference gas calorimeters in Europe to strengthen the whole system.

4. OBJECTIVES OF THE STUDY

The overall uncertainty of the calorific value measurement is coming for more than 90% from the temperature measurements in the calorimetric water bath. Hence, it is important to optimise thermal homogeneity and maximize heat transfer to the water bath by a combined experimental and modelling approach.

With this objective, LNE operated the experiments and Gaz de France performed a detailed transient 3D numerical simulation of the flow and heat transfer in the calorimeter bath, particularly checking the influence of the radiative heat transfer when compared to the imposed surface flux case, representative of the electrical heating during calibration.

We present here experimental water bath temperatures as a function of time during electrical heating and combustion of methane and results from the simulations with the CFD thermal model.

The numerical model adequately reproduces the experimental thermal behavior of the calorimeter. Consequently, after an experimental thermal characterization of the calorimetric bath, validated by numerical simulations, we present here a comparative study of the mean temperature evolution between experimental and numerical simulations.

The expected outcome of both experiments and thermal modelling is an improvement of the calorimeter performance in terms of uncertainty reduction.

5. EXPERIMENTAL AND COMPUTATIONAL SET UP

The calorimeter consists of a burner totally immersed in a water volume in which a given

quantity of gas is burnt. The heat released during combustion is transmitted to this water. The calorimetric vessel is thermally uncoupled from outside by the means of an enclosure (liquid stirred bath) maintained at constant temperature (isoperibolic aspect [2]). The calculation of the water temperature rise ΔT_{ad} representative of the temperature rise in an ideal adiabatic calorimeter allows an evaluation of the gas calorific value (GCV) thanks to eq (1):

$$GCV = \frac{C_{cal} \times \Delta T_{ad} + K}{m_{gas}} \quad (1)$$

C_{cal} is the heat capacity of the calorimeter determined by the electrical calibration ($J \cdot K^{-1}$), K is a corrective factor (J) and m_{gas} is the burned combustible mass (g).

All the temperature measurement elements of the system are very important: the sensor and its measurement system, the calibration of the probes as well as the process of measurements must be optimised because of the dominant weight of temperature uncertainty in the total gas calorific value uncertainty balance.

5.1 Experimental set up

The thermal characterisation of the calorimetric bath was performed with thermistor probes located at different sites in the bath and mounted on a grid located around the combustion chamber. Fig. 1 shows a sketch of the calorimeter assembly with the stirrer and its circulation tube and the burner. In the calibration mode, an electrical heating wire located around the burner (red wire in Fig. 1) provides the heat release. Joule effect dissipation simulates here the combustion heat release with a power of 61 W.

In the actual measurement operating mode, combustion with pure methane is performed to measure the energy released by the combustion of the known mass of gaseous fuel. A small sphere is filled initially with methane under pressure (20 bars approximately). The mass of the gas is determined by the double weighting method: the mass of the sphere is measured before and after the combustion.

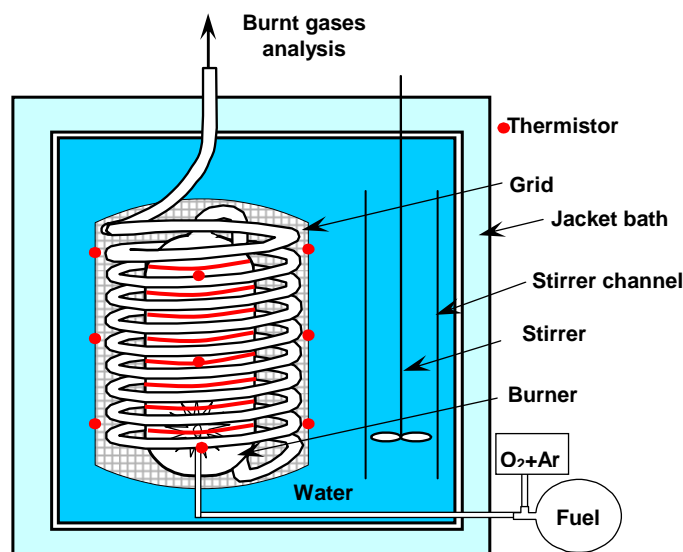


Figure 1: Sketch of the reference gas calorimeter. We visualise here 9 of the 12 thermistors

Thermistors were chosen to follow the bath temperature for their sensitivity (10 k Ω resistance in a glass-encapsulated material gives a sensitivity of 430 $\Omega/^\circ C$), their small geometry (1mm diameter of the bead) and their fast time response (1.5 seconds in an oil bath). The uncertainty of the thermistor calibration (done by comparison with a Standard Platinum Resistance Thermometer 25 Ω) was calculated to be $\sim 1mK$.

The following steps were performed experimentally:

1. Characterization of the calorimetric bath in terms of stability and homogeneity with a large set of thermistors;

2. Operation in the calibration mode with electrical heating with a set of thermistors or one thermistor;
3. Operation in the measurement mode with combustion with one thermistor.

Calibration and operation modes consist in three phases of 20 minutes each: the “fore phase”, during which the calorimeter is continuously stirred, and mean temperature experiences a small rise, the “main phase”, of heat input, either electrical or via combustion, and during which the mean temperature experiences the main rise, and the “after phase”, during which the heat contained in the burner is removed.

The single thermistor used in steps 2 and 3 was located at a specified point determined by the homogeneity experiments and the CFD simulations, as explained below.

5.2 CFD thermal model

The water volume inside the calorimeter bath is modelled with CFX thermal flow software. The objectives of this numerical study are the following:

1. To quantify the temperature distribution inside the water volume, in order to identify hot spots and some dead zones
2. To define best candidate zones for the temperature measurement, which are representative of the average water temperature
3. To study the influence of specific parameters on the thermal homogeneity and help minimise thermal scatter by choosing between several technical solutions.

The modelled domain is the water of the bath, with an accurate description of the complex geometry of the combustion chamber and exhaust coil. Water flows down in the recirculating channel, and then flows up along the combustion chamber and around the fumes exhaust coil - see Figure 2 for the unstructured mesh used in the calculations.

The geometrical representation of the small diameter pipe resulted in a very large mesh, around 700 000 nodes (Figure 2). This limited the modelling to steady state calculations in a first stage, but then transient calculations were also performed after optimising the model (around 450 000 nodes).

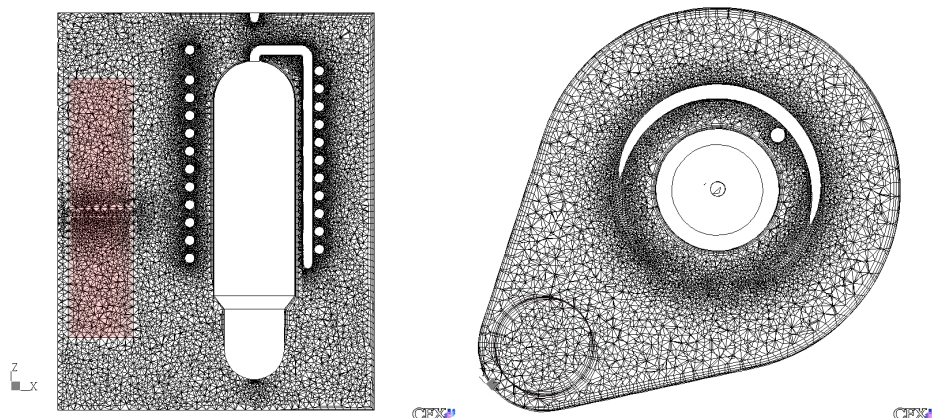


Figure 2: Vertical symmetry plane and horizontal (at about 3/4 of total height) cross-sections of the mesh.

While the first step of the experimental study concerns bath stability and homogeneity tests during electrical dissipation, numerical simulations make sense mainly with thermal power release. The thermal load was estimated at 61 W. It is supposed to be a uniformly distributed flux along the combustion chamber in the calibration mode, and as a bracketing approach for the measurement mode, a radiative flux distribution is imposed, with axial symmetry, and decaying with increasing height of the burner surface.

The thermal boundary condition on the outside wall and jacket side is matched with a simplified approach of an equivalent material, representing the multi-layer structure of the two metal walls, the air inside the gap, and the water circulation outside the jacket.

Water is circulated inside the bath via a momentum source located at half-distance of the recirculating channel. The value of this source was adjusted to obtain a certain recirculating velocity, defined as the average velocity in this channel. The value of recirculating velocity used at this stage was 30 cm/s according to experimental evaluation.

In the case of radiative transfer, the properties of water were assumed for the sake of simplicity to be that of a grey medium, with an equivalent absorption coefficient.

The grid where the thermistor probes are fixed in the experiments is not represented.

6 EXPERIMENTAL AND NUMERICAL RESULTS

6.1 First experimental results:

The calorimetric water bath was characterized during thermal stability tests and also during electrical heating test with the 12 thermistors installed in the bath and described previously. The jacket temperature was maintained at 25°C and the stirrer rotation speed was 600 rpm. This optimised stirrer speed was evaluated with a high-speed camera. At this speed, the water velocity in the outflow of the stirrer channel was evaluated at about 30 cm/s. The power dissipated by the stirring was measured to be 0.39 W during stability tests. The electrical heating power was 50 W.

The temperature evolution profiles are presented in Fig. 3.

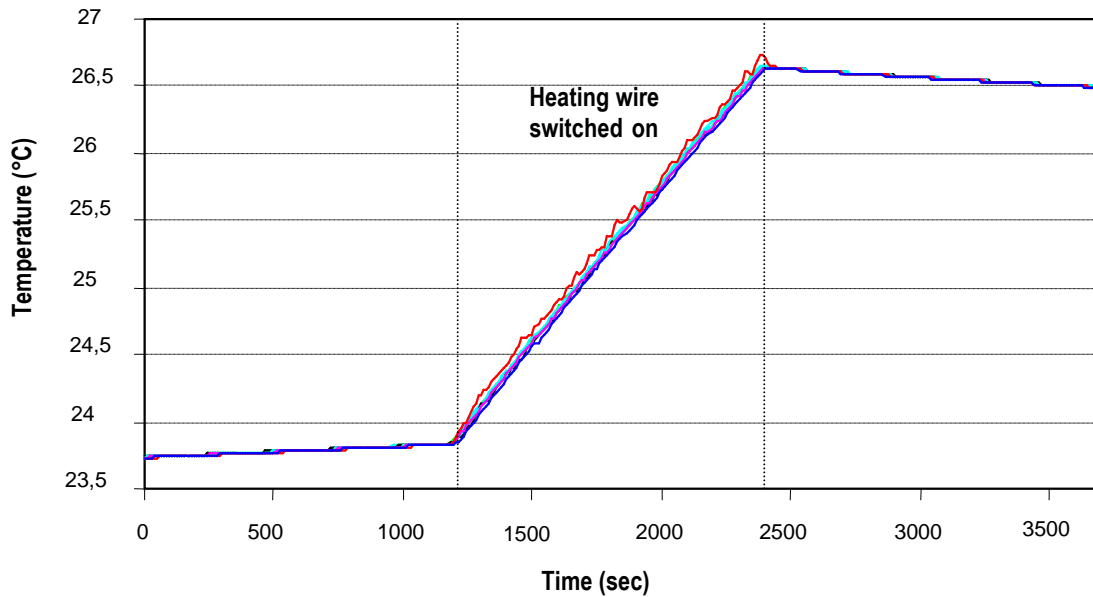


Figure 3: Temperature profiles with 12 thermistors during electrical heating

The different results on temperature rise and thermal homogeneity are summarized in the following table:

Experimental temperature rise	2.7713 K
Standard deviation due to inhomogeneity in the water bath	1.4 mK in the quasi-stable phases (fore and after phases)
	32.3 mK in the dynamic regime (heat release phases)

Table 1: Results from thermal stability of the water bath experiments.

We can observe a slight temperature increase during the quasi-stable phases. In the fore period, the increase is about 140 mK and in the after period, it is evaluated at 130 mK, these values for 20 minutes each. This deviation is due to heat released by the stirring, to the environment temperature (jacket temperature at 25°C and room temperature at 23°C). Some long-term stability tests have been

performed in the past at a stirrer speed of 250 rpm and a slight temperature increase of around 40 mK has been observed during 8 hours (at 31°C). This confirms that thermal environment conditions have a significant influence on the deviations obtained previously.

6.2 Average temperature evolution

The first experimental and numerical results showed that the position of the single sensor to be used for average water bath temperature measurement is critical and needs to be precisely defined. An optimised location for the thermistor was found, between the burner and the vessel wall at the opposite side of the stirrer close to calorimeter mid-height. The numerical simulations helped validate this thermistor location, as seen below.

The next step was to compare experimental and numerical results on similar configurations. Same input data were applied to both experiments and numerical simulations, for both operating modes: calibration, i.e. electrical dissipation modelled via convective power release, and GCV measurement, i.e. combustion energy release modelled via a pure radiative power release.

In the calibration mode, a power of 61 W was released via electrical heating during 20 minutes. The average temperature curve measured with one thermistor is presented in Fig. 4. The blue curve represents the voltage applied to the heating wire (resistance of 34.87 Ω). The temperature rise during the heating period is around 3.76 K. A slight temperature increase is observed in the fore period, due to the temperature difference between bath (initially at 23°C) and jacket temperature, at 27°C, as well as to the stirrer energy dissipation. In the after period, a smaller temperature increase is also visible, due mainly to stirring.

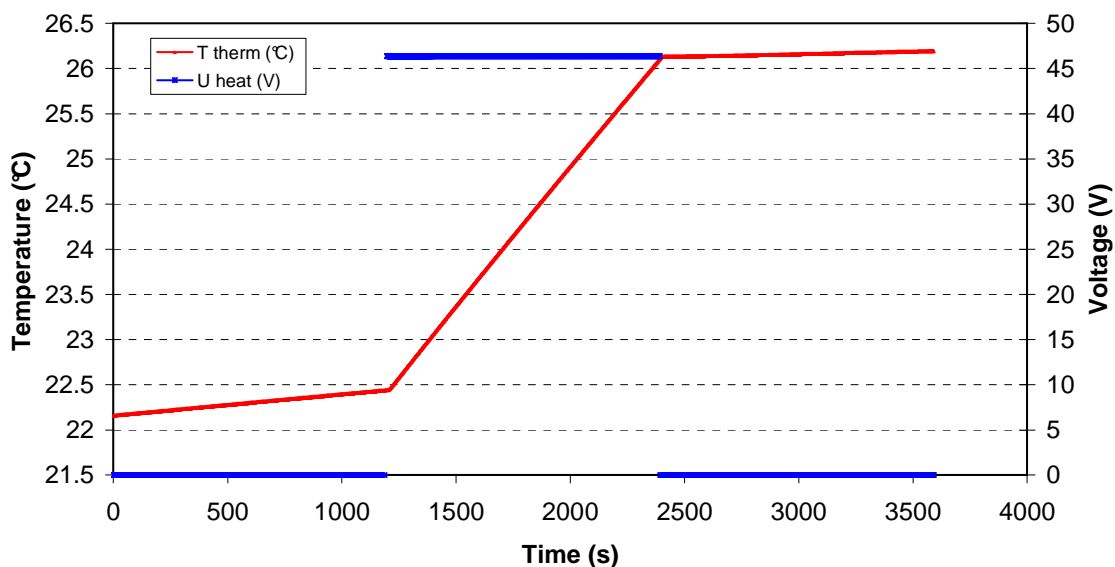


Figure 4: Experimental calibration mode via electrical heating (61 W): Thermistor temperature evolution, representative of the mean temperature evolution, and heating resistance voltage.

The results of the corresponding numerical simulation case appear in Fig. 5. The advantage of numerical simulation is that more information is available, so not only average temperature values are given, but also the local temperature at the thermistor location, minimum and maximum temperatures in the modelled water bath.

The most outstanding findings are: average temperature increase is about 4.3°C, and thermistor location temperature differs from average bath temperature only by a maximum of 20 mK, which is below the accuracy of modelling. Minimum temperature is also very close, only the maximum bath temperature exhibits an excursion of about 8.54 °C, which indicates a very localised effect close to the top of the combustion chamber. The difference in average temperature increase, 0.54°C, needs

to be checked with a repetition of the test, as well as with an improvement in the boundary conditions of the numerical model. It remains still very small compared to the usual applications of numerical modelling.

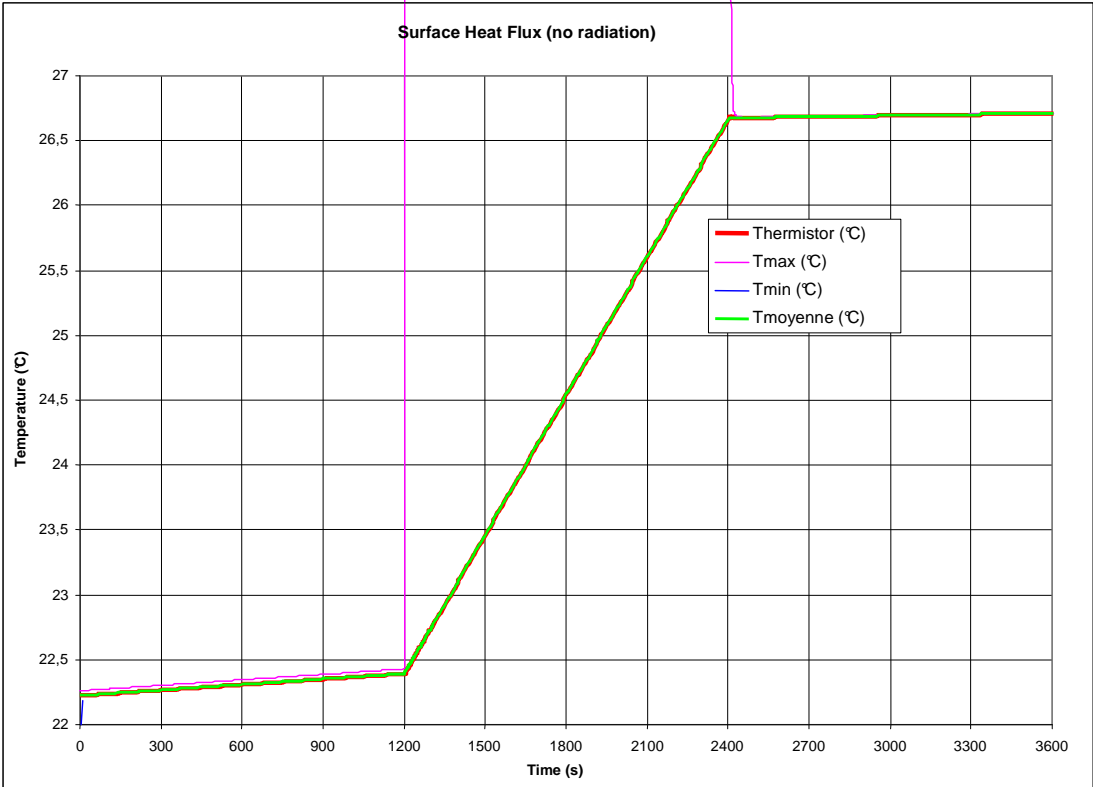


Figure 5: Numerical simulation results for the calibration mode: average, minimum, maximum, and thermistor temperatures evolutions during the 3 phases.

A similar comparison was established for the measurement operating mode. We performed combustion of methane (purity 5.5), oxygen (5.8) and argon (6.6) during 20 minutes approximately and the fuel gas flow was calculated to obtain a total power release of 61 W (91 ml/min). The gas mixture is a lean one and argon allows stabilizing the flame. The jacket temperature is 27°C and the room temperature is 23°C. The average bath temperature curve is presented in Fig. 6, with the methane flow represented by the blue curve. The thermistor temperature rise is about 3.95°C.

The corresponding numerical results are plotted in Fig. 7, for the same conditions, with the specific simplified treatment of a pure radiative heat release at the outside surface of the burner. The main findings are: the average temperature rise for this idealised case of a pure radiative source is very similar to the calibration case, i.e. about 4.3°C; unlike the calibration case, in this case radiative heat transfer plays a strong role in increasing bath homogeneity, as the maximum temperature is predicted to be only 1.17°C above the average bath temperature, a lot less than in the calibration case. This justifies the design choice of a transparent burner, which helps transferring heat directly to the water bath rather than using the conductive coupling through the burner wall, as occurs in usual applications.

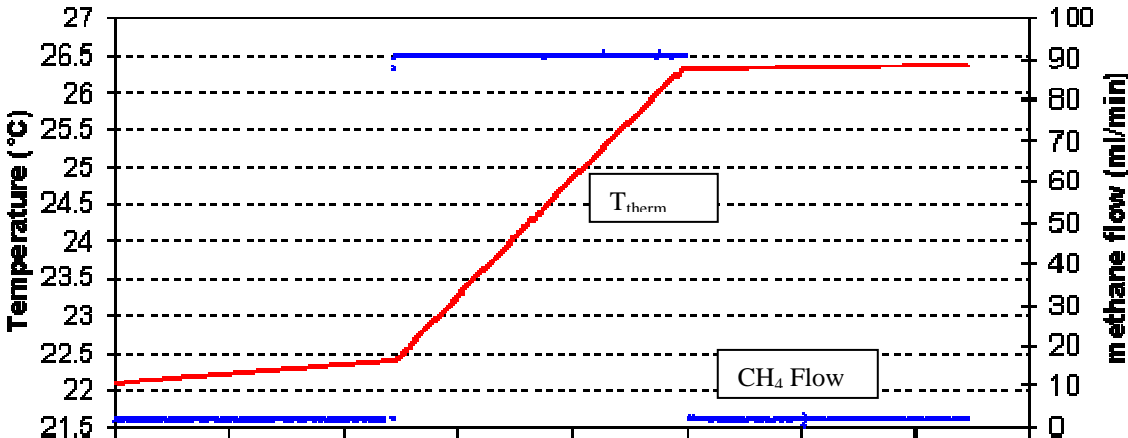


Figure 6: Measurement mode with methane combustion: thermistor temperature and methane flow rate evolution vs. time.

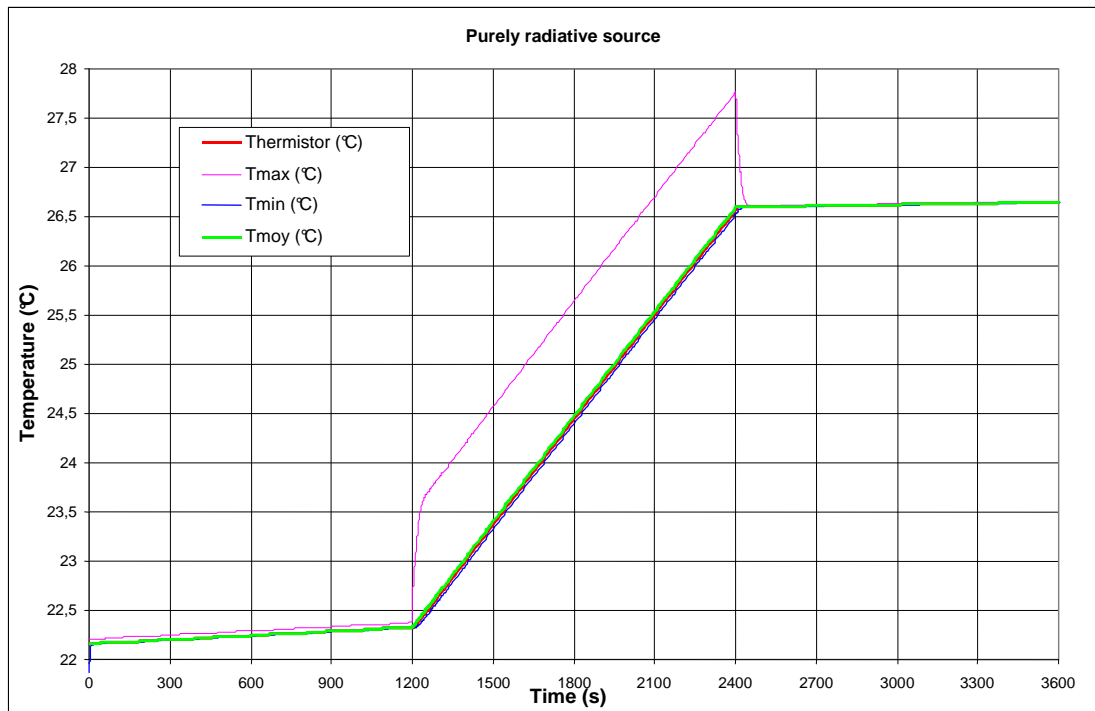
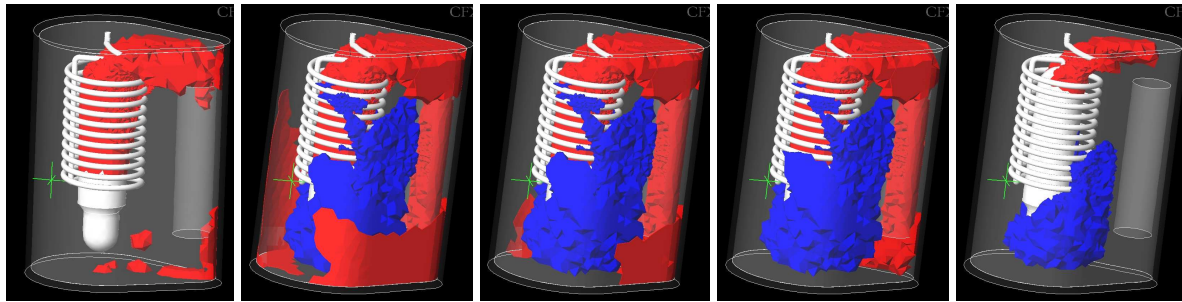


Figure 7: Numerical simulation results for the measurement mode with a pure radiative source: average, minimum, maximum, and thermistor temperatures evolutions during the 3 phases.

6.3 Single thermistor position for measuring average bath temperature

The issue of positioning the thermistor so as to ensure a measurement that represents well the average bath temperature can also be addressed via numerical simulation. We developed an approach that visualises the water bath volume that is either hotter or colder than the average temperature, by a predetermined amount, e.g. 0.05°C . For illustration purposes, we present here only the worst case, representative of the calibration mode, where thermal non-homogeneities are at their highest. In Fig. 8, we present an example of a series of successive views of the water bath thermal field, on which the red areas (upper half of the domain) are hotter by at least 0.05°C than the average temperature, while the blue areas are at least colder by 0.05°C than the average temperature. That means that in the rest of the domain, which remains transparent, the water temperature is bracketed by $T_{\text{average}} \pm 0.05^{\circ}\text{C}$. The region that remains “transparent” on these figures throughout the whole process is the most appropriate location for a thermistor that is supposed to measure an average temperature. Such a region was identified, and the green cross shows the best location for the thermistor according to the numerical model. This finding was also confirmed by experimental evidence; therefore the location of the thermistor was optimised.



$t = 1210 \text{ s}$ $t = 1300 \text{ s}$ $t = 1800 \text{ s}$ $t = 2400 \text{ s}$ $t = 2410 \text{ s}$
Figure 8: Volumes characterised by a temperature difference $\geq 0,05 \text{ K}$ (red) or $\leq 0,05 \text{ K}$ (blue) with respect to average temperature at time t (combustion starts at $t = 1200 \text{ s}$ and ends at $t = 2400 \text{ s}$)

Numerical modelling can be used also in other ways to optimise the design of the reference calorimeter, and such complementary actions are now underway, to help achieve the very ambitious goal that was set in the beginning for the accuracy of the reference calorimeter.

7. CONCLUSION

An overview of the rapidly changing environment in the gas industry showed that delivered energy needs to be known at an increasing number of points in the networks, with specified levels of accuracy, and of course, with the constraint of least cost. As mainly indirect methods are used to evaluate this energy content, there is a need for improved reference gas calorimeters, which are able to quantify the energy content of fuel gases with an accuracy of less than 0.1 %. The anticipated uses for such a reference calorimeter were clearly identified.

Reducing measurement uncertainty linked to the thermal non-homogeneity in the calorimetric bath was identified as a key point to control in order to achieve the ambitious goal set for the reference calorimeter, an accuracy on GCV of 0.05%.

Therefore, within the framework of a European collaborative project led by GERG, LNE and GDF R&D Division focused on an approach mixing experimental and numerical simulation in order to optimise the design of a reference calorimeter for France.

First experimental results helped characterise thermal bath stability without heating, as well as part of the spatial non-homogeneity.

Subsequent experiments led both in calibration mode, with energy release based on electrical heating, as well as measurement mode, with energy release due to fuel gas combustion, were compared favourably to numerical simulations. The main finding is that thermal non-homogeneity is larger in the calibration mode than in the measurement mode, so this point needs some more work. In addition, using numerical simulation, and confirmation by tests, an adequate location was found for the thermistor probe, which is supposed to measure the water bath average temperature. More realistic numerical models will help advance and optimise the design of this reference calorimeter even further.

REFERENCES

- [1] ISO 6976:1995, (1995). Natural gas - Calculation of calorific values, density, relative density and Wobbe index from composition, Geneva: International Organization for Standardization, 46p
- [2] Rossini, F.D., (1931). The heat of formation of water, *National Bureau of Standards*, **6**, pp. 1-35
- [3] M. Jaeschke, R. Forster, A. Schmücker, F. Haloua, B. Hay, V. Le Sant, S. Loubat, D. Laguerre, A. Benito, P. L. Cremonesi, (2004). GERG Project : Development and set-up of a new reference calorimeter, International Gas Research Conference, Vancouver, Canada.

List of tables:

Table 1: Results from thermal stability of the water bath experiments.

List of figures

Figure 1: Sketch of the reference gas calorimeter. We visualise here 9 of the 12 thermistors

Figure 2: Vertical symmetry plane and horizontal (at about 3/4 of total height) cross-sections of the mesh.

Figure 3: Temperature profiles with 12 thermistors during electrical heating

Figure 4: Experimental calibration mode via electrical heating (61 W): Thermistor temperature evolution, representative of the mean temperature evolution, and heating resistance voltage.

Figure 5: Numerical simulation results for the calibration mode: average, minimum, maximum, and thermistor temperatures evolutions during the 3 phases.

Figure 6: Measurement mode with methane combustion: thermistor temperature and methane flow rate evolution vs. time.

Figure 7: Numerical simulation results for the measurement mode with a pure radiative source: average, minimum, maximum, and thermistor temperatures evolutions during the 3 phases.

Figure 8: Volumes characterised by a temperature difference $\geq 0,05$ K (red) or $\leq 0,05$ K (blue) with respect to average temperature at time t (combustion starts at $t = 1200$ s and ends at $t = 2400$ s)